IOSR Journal of Computer Engineering (IOSR-JCE)
e-ISSN: 2278-0661, p-ISSN: 2278-8727, Volume 27, Issue 4, Ser. 1 (Jul. – Aug. 2025), PP 24-49
www.iosrjournals.org

Analysis of State of Charge (Soc) Estimation Algorithms for Lithium-Ion Batteries Compared with Feedforward Neural Network

Farnaz Nawaz[1], Muhammad Qasim Shah[2], Muhammad Sarwar Ehsan[3], Qulsum Asif[4], Abdul Wajid[1], Maleeha Shafique[5], Muhammad Idrees[6]
[1]*Institute of Electrical, Electronics & Computer engineering, University of the Punjab, Pakistan.*
[2]*Faculty of Science and Technology, Bournemouth University, England, United Kingdom.*
[3]*Faculty of Information Technology & Computer Science, University of Central Punjab, Pakistan.*
[4]*Department of Physics, Government College University, Pakistan.*
[5]*Center for Advance Studies in Physics, Government College University, Pakistan.*
[6]*Department of Electronics, Government College University, Pakistan.*
Corresponding author: mqasim@bournemouth.ac.uk

Abstract
Lithium-ion battery cells play a critical role in meeting the rising demand for electric vehicles (EVs) due to their superior nominal voltage, energy density, extended cycle life, and high-power capacity. Among the key parameters for assessing battery performance, the State of Charge (SOC) serves as a vital indicator of a battery's available capacity and ensures the safe and efficient operation of EVs. Accurate SOC estimation is essential for effective Battery Management System (BMS) functionality. This study proposes an Enhanced Equivalent Circuit Model (ECM) combined with Kalman Filter (KF)-based techniques to improve SOC estimation accuracy in EV batteries, as compared to traditional Feedforward Neural Network (FNN) data-driven methods. The methodology begins with the development of a second-order RC ECM to characterize lithium-ion battery behavior. Battery operational parameters—including terminal voltage, load current, and temperature—are measured to establish baseline values for SOC estimation. These measurements ensure compliance with safety standards during charge-discharge cycles. Subsequently, the Kalman Filter (KF), Extended Kalman Filter (EKF), and Unscented Kalman Filter (UKF) are applied to minimize SOC estimation errors and boundary deviations. Results demonstrate that the KF and EKF algorithms maintain SOC boundary errors within ±2.4% while achieving estimation errors below 1.6%. However, the UKF outperforms both, yielding a reduced estimation error of 0.4% and a boundary error of 1.4%, highlighting its robustness against measurement noise and operational uncertainties. Further validation reveals that the UKF approach achieves an exceptionally low Root Mean Squared Error (RMSE) of 0.01%, ensuring high precision. For comparative analysis, an FNN trained over 200 epochs with three repetitions achieves an RMSE of 0.03%, confirming its viability but with marginally lower accuracy than the UKF. In summary, the proposed filtration-based SOC estimation method proves more reliable than data-driven techniques, with the UKF improving Simulink model accuracy by 0.39% over conventional methods, while the FNN enhances precision by 0.37%. These findings underscore the efficacy of model-based filtering strategies for precise SOC determination in EV applications.
Keywords: *Battery Management System (BMS), Equivalent Circuit Model (ECM), Unscented Kalman Filter (UKF), Extended Kalman Filter (EKF), Kalman Filter (KF), EV applications.*

Date of Submission: 04-07-2025 Date of Acceptance: 14-07-2025

I. Introduction

In Since lithium-ion batteries have a big capacity, a high energy density, a long lifespan, and are easy to control and operate, they have been widely used in electric cars. One of the most important criteria for enhancing Li-ion battery performance in electric vehicles is state of charge (SOC). Accurate SOC calculation is necessary to manage Li-ion batteries efficiently and guarantee their longevity by preventing over-discharge. Since SOC relies on observable components, it is challenging to measure them directly. As a result, a precise SOC estimation technique is necessary. This thesis aims to provide a clear and accessible explanation of a precise SOC estimation method with an emphasis on lithium-ion batteries. To preserve battery health and operational safety, accurate SOC estimation is essential. As a result, electric vehicles will perform better and have longer battery life **[1]**.

There are several models and techniques available for calculating SOC, including those for electrical circuits, PDEs, hybrids, direct measurement, and accounting systems. These methods, however, have limitations that make it challenging for them to produce accurate SOC estimations. Filtering techniques stand out as a suggested choice among them because of their capacity to reduce noise in internal parameter estimation, which is a crucial part of ensuring safety in electric vehicles. Kalman filters are often utilized in linear system SOC estimates. Given the prevalence of non-linear systems, two variants of Kalman Filter (KF) have been developed to improve the accuracy of lithium-ion battery SOC calculation: Extended Kalman Filter (EKF) and Unscented Kalman Filter (UKF). One important component of the KF's effectiveness is the model's accuracy in identifying the battery properties needed for the SOC calculation.

Adaptive filters are dynamic techniques that constantly adjust their settings to account for shifting battery behavior. This flexibility enhances SOC estimation, especially when non-linear battery characteristics and a range of operating situations are present. One type of adaptive filter is the LMS (Least Mean Squares) algorithm. The mean squared error between their estimations and the actual data is reduced, making them valuable tools for real-time applications. SOC is estimated using RLS (Recursive Least Squares), NLMS (Normalized LMS), and Sign-Sign LMS, which are variations of the LMS (Least Mean Squares) filter.

These filters offer multiple methods for precisely tracking state of charge (SOC) in battery management systems by adjusting to different system dynamics and non-linear situations. Changing to a more contemporary method will work.

Nomenclature

C	capacity of cell (Ah/mAh)	V_{oc}	the Open Circuit Voltage
I_t	current defined as I_t(A) = rated capacity (Ah) / 1(h)	R0	battery ohmic resistance (Ω)
I_L	current drawn by load (A)	***Abbreviations***	
V_t	terminal voltage of battery (V)	EV	Electric Vehicle
T	temperature (°C)	CC	Coulumb Counting
C_1,C_2,C_3	the polarization capacitances (F)	SOH	State of Health
R_1,R_2,R_3	the polarization resistance (Ω)	C-rate	Charging /Discharging rate
Greek letters and symbols		Li-ion	lithium-ion battery
–	mean value	ECM	State of Function
^	estimated value	DOD	Depth of Discharge
~	error (residual) value	SVM	Support Vector Machine
T	transpose operator	RUL	
	Remaining Useful Life		
R	sampling points/sigma points		
i	information content		
S	distribution of sigma set		
p	probability distribution function		
c	auto-correlation function		

a	status vector	PDE	Partial Differential Equation
e	system noise vector/process noise	OCV	Open Circuit Voltage
c	system control vector	LSTM	Long Short Term Memory
d	observation noise vector	FFNN	Feed-Forward Neutral Network
G	filter gain	MAE	Mean Absolute Error
b	observation vector	RMSE	Root Mean Square Error
k	sample time	MAX	Maximum Error
E[ ]	expected value	HEV	Hybrid Electric Vehicle
E_{xx}[ ]	covariance	KF	Kalman Filter
E[ǀ]	conditional probability	EKF	Extended Kalman Filter
β	weight for the UKF computations	UKF	Unscented Kalman Filter
m	mode number in UKF		

Feedforward Neural Networks (FNNs) enhance State-of-Charge (SOC) estimation by processing input data through multiple hidden layers, adjusting connection weights iteratively to minimize prediction errors. This enables accurate modeling of complex battery behavior patterns.

Developing reliable SOC estimation algorithms remains critical for optimizing electric vehicle (EV) battery performance. This work addresses the nonlinear dynamics of lithium-ion batteries by comparing FNN data-driven approaches with Unscented Kalman Filter (UKF)-based adaptive filtering, aiming to improve estimation accuracy and robustness across operational conditions.

II. Literature Review

An outline of the many kinds of electrochemical batteries and their characteristics can be found in the introduction to Section 2.1. In Section 2.2, various methods for estimating SOC are examined, along with their uses, disadvantages, and restrictions. A brief description of how to use model-based techniques to estimate the state of charge (SOC) of lithium-ion batteries in electric vehicles (EVs) is given in Section 2.3. A brief overview of the categorization of filtering techniques is provided in Section 2.4. The use of the Least Mean Square Algorithm and its variations is introduced in Section 2.5. In Section 2.6, we finally examine a different method for estimating SOC that makes use of feedforward neural networks.

2.1 Introduction

Since batteries are necessary for many multimedia-based devices, their use is growing globally. One of the primary issues with the increasing demand for batteries is ensuring their reliability and calculating their lifespan to achieve the best possible energy efficiency **[2–3].** Our increasing reliance on batteries has led to advancements in battery technology, with a focus on characteristics like memory-free functioning, high energy density, small size, and long lifespan. Of all the battery types that are currently accessible, lithium-ion batteries are the most widely used. These batteries are ideal for a range of gadgets and applications, including solar street lighting, power tools, medical equipment, power trains, cameras, laptops, and cell phones, because they are more efficient and rechargeable than their counterparts. Because lithium-ion battery life is dependent on how they are charged and discharged, it is extremely difficult to predict **[4]**. After being fully depleted, a battery won't last very long. Therefore, it is crucial to conduct study on battery longevity prediction.

2.1.1 Classification of Batteries

Since batteries are necessary for many multimedia-based devices, their use is growing globally. One of the primary issues with the increasing demand for batteries is ensuring their reliability and calculating their lifespan for the best energy efficiency **[5]**. The exponential rise of batteries in portable electronic devices such as computers, laptops, and mobile phones, as well as their ubiquitous use in electric cars and businesses, has spurred ongoing study and technological advancements. Because of this, these technologies have advanced significantly and are now widely used **[6]**. Batteries are frequently categorized according to a number of factors, including size, lifetime, and chemical makeup **[7-8]**.

There are some basic battery types.

- Physical battery
- Solid state battery **[9]**
- Bio battery **[10-11]**
- Electrochemical battery
- Supercapacitors
- Flow battery
- Lithium-Polymer (Lipo)
- Zinc-Air battery
- Sodium-Ion battery
- Fuel cells

Figure 2.1 offers further classification of these batteries.

Because of their exceptional efficiency, electrochemical batteries are the best option among these battery types for electric cars and are strongly advised for use in a variety of application scenarios.

2.1.1.1 Electrochemical Batteries

When compared to other battery technologies, electrochemical batteries offer excellent performance, elevated energy density, and greater efficiency in electric cars, making them a suitable choice for the future generation **[12]**. An electrochemical battery pie graph is shown in **Figure 2.2**.

Depending on their chemical makeup, electrochemical batteries can be divided into primary and secondary varieties. Once fully depleted, primary batteries cannot be recharged and are not used.

Examples of secondary batteries include the following battery types:

- Lithium-ion (Li-ion)
- Nickel-metal hydride (NiMH)

- Nickel-cadmium (NiCd)
- Lead-acid

Unlike nickel and lead acid batteries, lithium-ion batteries are frequently used as electrochemical energy storage devices **[13–15]**. Because of its greater capacity, lighter weight, and better energy density, lithium-based technologies are primarily used in electric vehicle batteries (EVBs). Lithium-ion batteries are a better option for EV applications, as evidenced by their performance characteristics, which include nominal voltage, life cycle, efficiency, and energy capacity **[16]**.

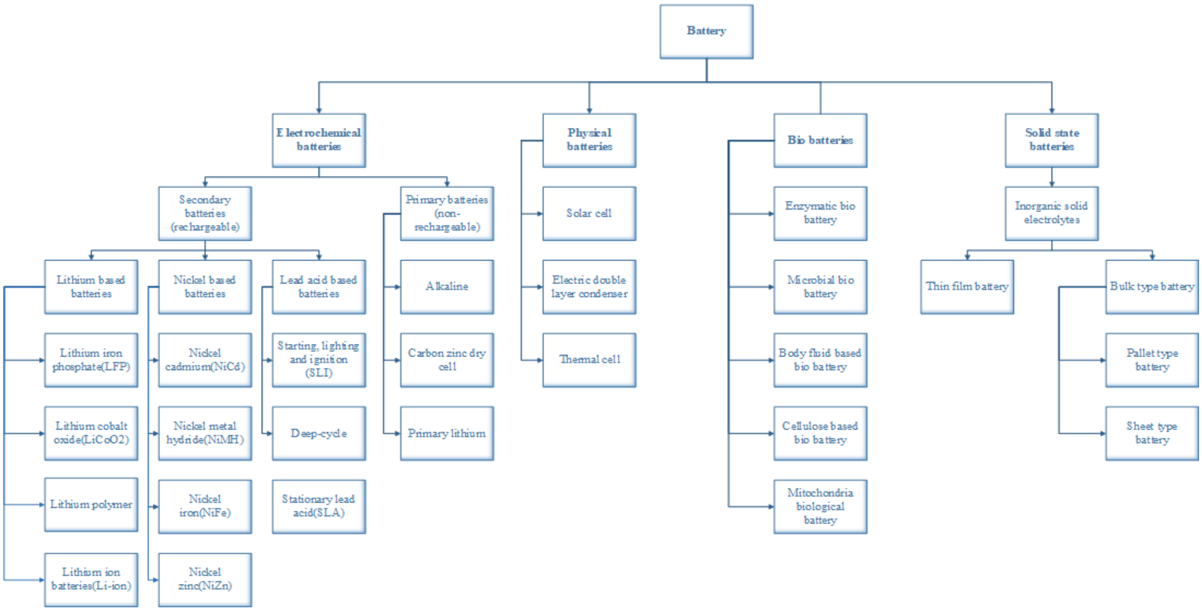

Fig. 2.1: Categorization of batteries

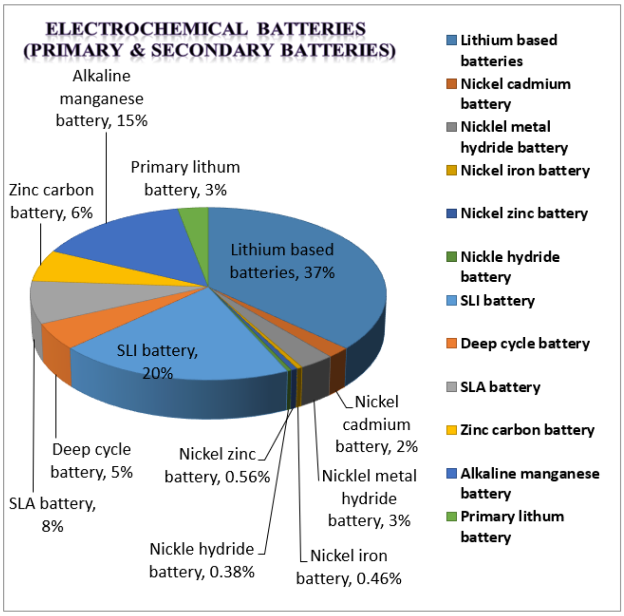

Figure 2.2: Pie graph of the electrochemical batteries

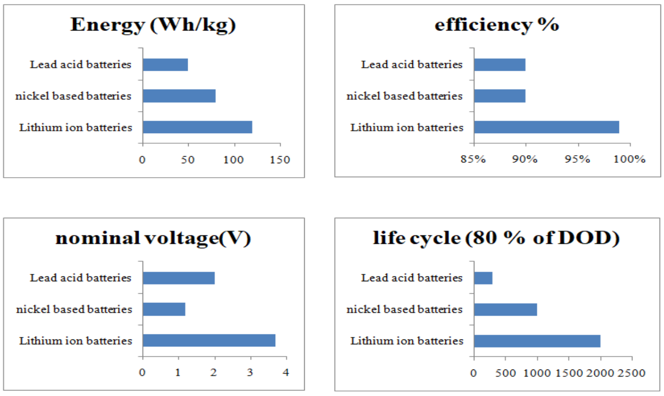

Figure 2.3: Features of several EV batteries

2.1.1.2 Lithium-ion Secondary Battery

Lithium-ion batteries stand out from other rechargeable options like lead-acid and nickel-based batteries, thanks to their superior performance and reliable recharging capabilities shown in **Figure 2.3.** Among these advantages are its high energy density, minimal maintenance requirements, extended lifespan (more than 2,000 cycles), memory-effect-free design, increased capacity, and dependable performance at high temperatures. Due to its many advantages, particularly in the electric vehicle (EV) sector, lithium-ion battery utilisation has been growing quickly all over the world **[17-18]**.

2.1.1.3 Application of Lithium-ion Battery as Electric Vehicle

Lithium-ion batteries have become indispensable in modern technology, powering everything from portable electronics to electric vehicles and renewable energy systems. Their widespread adoption stems from superior energy density and longevity, making accurate State of Charge (SOC) estimation critical for battery management and operational safety. Precise SOC determination ensures reliable performance monitoring, safeguards battery health, and optimizes remaining capacity utilization in electric vehicles.

2.2 SOC Estimation for Electric Vehicles

Accurate State of Charge (SOC) estimation is critical for lithium-ion battery performance in electric vehicles, directly impacting energy efficiency, safety, and lifespan by preventing overcharge/discharge **[19–20].** While methods like electrochemical models and circuit-based approaches **[21–31]** have advanced SOC estimation, operational factors like temperature and aging complicate real-world accuracy. This section evaluates these techniques and their role in optimizing EV battery management systems.

2.3 Method of State for Charge (SOC) Estimation

Several SOC estimate techniques are listed below:

- Direct Measurement
- Model-based method
- Indirect estimation methods
- Trained data estimation method
- Hybrid method

Additionally, **Figure 2.4** shows how the approaches are divided.

2.3.1 Direct Measurement Method

Types of methods are:

- Open circuit Method (OCV)
- Terminal Voltage Method
- Impedance spectroscopy

These techniques utilise the physical characteristics of batteries, including their impedance ('z') and terminal voltage ('v'). Measurement of battery temperature "T" is also necessary for estimating SOC because these quantities rely on temperature.

$$\mathrm{SOC} = \int_{\mathrm{T}}^{\mathrm{d}} (\mathrm{v}, \mathrm{z}) \qquad (2)$$

The relationship between OCV and SOC varies amongst batteries, despite being nonlinear in the context of lithium-ion batteries due to the unreliability of SOC estimation **[32–33]**. Nevertheless, the terminal voltage method requires accurate voltage readings, which are not accessible **[34]**. When employing the impedance spectroscopy method, expensive equipment is needed to estimate SOC.

2.3.2 Indirect Measurement Method

1-Book-keeping Method

Accurately estimating SOC via direct methods is challenging. To address this issue, engineers have created indirect procedures known as "book-keeping estimation methods," which are described in reference **[35].**The most popular of these methods is the coulomb counting method, which primarily relies on measuring and integrating current.

2-**Coulomb counting method**

The coulomb counting method analyzes a battery's discharge current and integrates the terminal current to estimate SOC **[36].**

$$SOC = \int_{T}^{t}(i)dt \qquad (3)$$

However, the Coulomb counting is simple to employ. The discontinuous integration of current limits the accuracy of the SOC estimation and results in mistakes in the discharge current and battery lifespan calculations.

2.3.3 Hybrid Method

Hybrid methods improve SOC accuracy by combining complementary approaches - notably coulomb counting with either EMF analysis or Kalman filters - while remaining sensitive to initial conditions and aging effects **[37-40]**. Estimation methods are listed in **Table 1**.

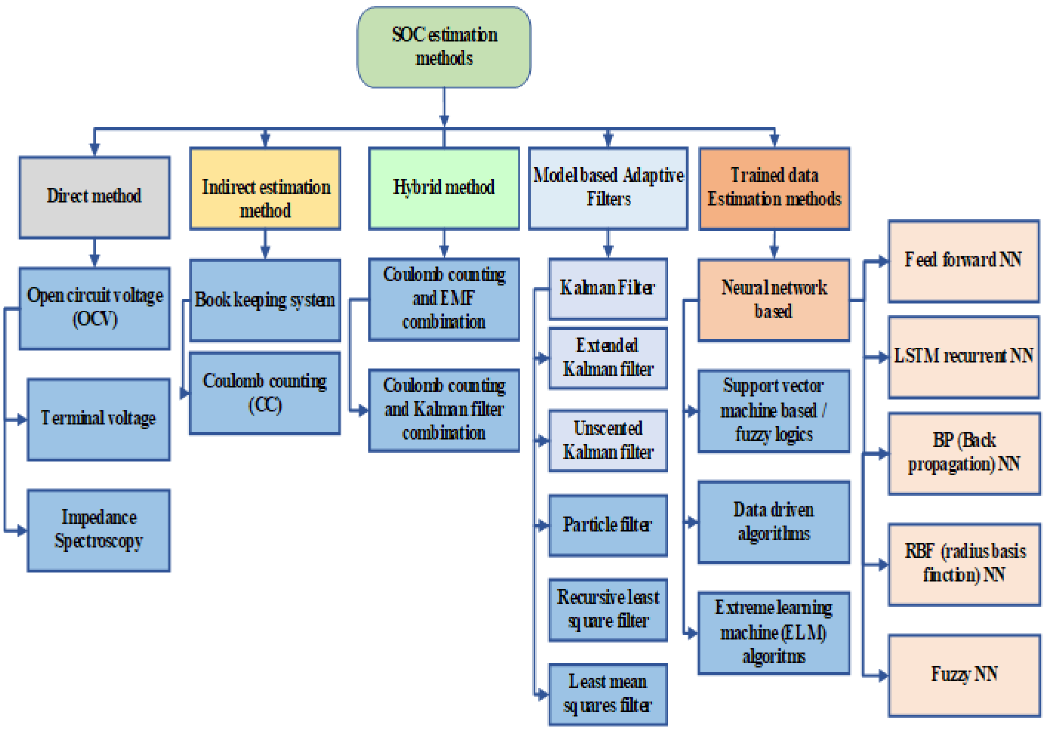

Figure 2.4 Sub Division of SOS estimate methods

2.3.4 SOC Estimation Methods Comparison

Table 1: comparisons of various SOC estimate techniques:

Method	References	Input Parameters	Advantages	Disadvantages	Accuracy
Model-based Filtering	Wang, 2019 **[41]**	Battery model, self-discharge rate, starting SOC value, terminal voltage, and terminal current	Precise, closed-loop, noise-insensitive, can handle errors in starting SOC value	Computationally expensive, highly dependent on the accuracy of the battery model	Max < 0.8%, Mean < 0.4%
Hybrid	Xia et al., 2018 **[42–43]**	Terminal temperature, current, and voltage	Accurate, highly precise if model is correct	Complex, requires highly accurate input variables	Maximum error: 3.5%
Indirect Estimation	Xia et al., 2018 **[44]**	Current, Temperature	Input parameters are easily obtainable	Susceptible to error accumulation, leading to unreliable estimates	Maximum error: 3%
Direct Measurement	Zhang et al., 2018 **[45]**	Terminal voltage, impedance, temperature	Simple, low computational demand, minimal mathematical modeling	Open-loop, sensitive to sensor accuracy	Maximum error: 1.5%

2.4 Model-based Filtering Method

Kalman filters are the go-to tool for battery state estimation—noisy data is no match for them. Since their debut in 1960 **[46-47]**, they've been a game-changer for EVs, cleaning up messy signals like a pro shown in **Figure 2.5**. But batteries don't play by linear rules, so researchers leveled up with Extended and Unscented Kalman Filters. These smarter versions handle the twists and turns of real-world battery behavior **Figures. 2.6-2.7**, constantly fine-tuning their predictions to nail SOC estimates in real time**. Figure 2.8** shows working of Kalman filter with battery model.

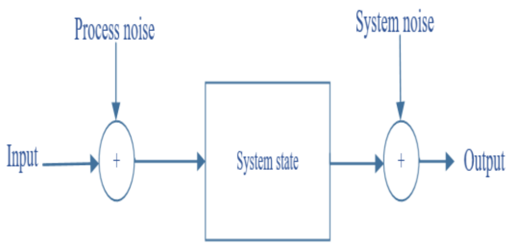

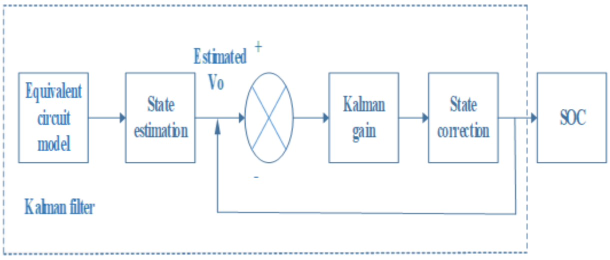

Figure 2.5: Noise reduction in battery systems using filtering techniques Figure 2.6: State of Charge (SOC) prediction using recursive Kalman filtering

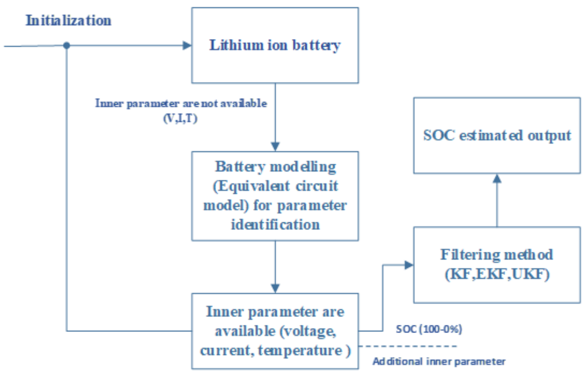

Figure 2.7: Real-time SOC tracking algorithm for EV batteries with noise filtering

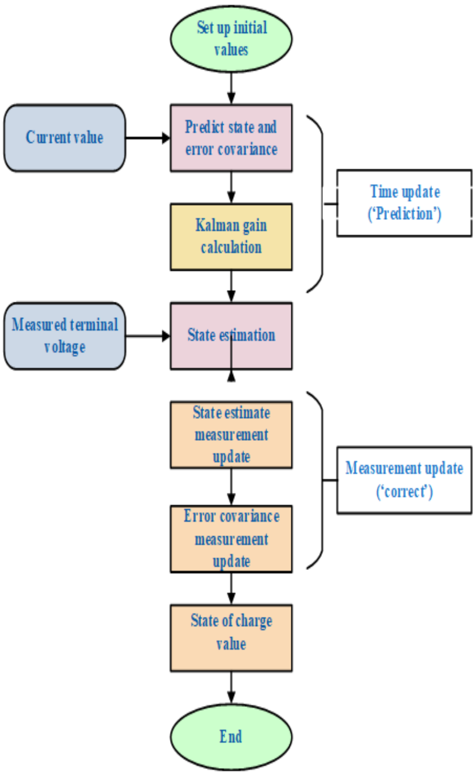

Figure 2.8: Smart SOC Prediction - How Battery Models and Kalman Filters Work Together

2.4.1 Modeling of Battery for Parameter Identification

Utilizing an effective battery model is essential when using filtering techniques for parameter identification in order to obtain an accurate State of charge (SOC). In practical applications, the internal SOC is closely linked to external variables like as temperature, voltage, current, and a number of other characteristics. Numerous battery models are used to determine battery parameters, comprising partial differential equation (PDE) models, Thevenin circuit models, Coulomb counting models, Open Circuit Voltage (OCV) models, and mathematical models. Among the different modeling approaches, the Equivalent Circuit Model (ECM) is a highly recommended choice because it is simple to identify parameters and has no effect on the basic characteristics of the battery. As a result, the best choice for determining battery state of charge (SOC) is ECM.

2.4.1.1 Equivalent Circuit Model

One important instrument in the field of battery modeling is the Equivalent Circuit Model (ECM). It simplifies the intricate electrical behavior of batteries by using basic electrical components such as resistors, capacitors, and voltage sources. Due to its accuracy and usefulness, this modeling approach has gained a lot of traction in the market and is now a mainstay for figuring out crucial battery characteristics including temperature, terminal voltage, current, and beginning parameters for the filtering process.

2.4 Filtering Method Categories

Figure 2.9 presents the classification of filtering approaches used in SOC estimation, highlighting their relationships and applications.

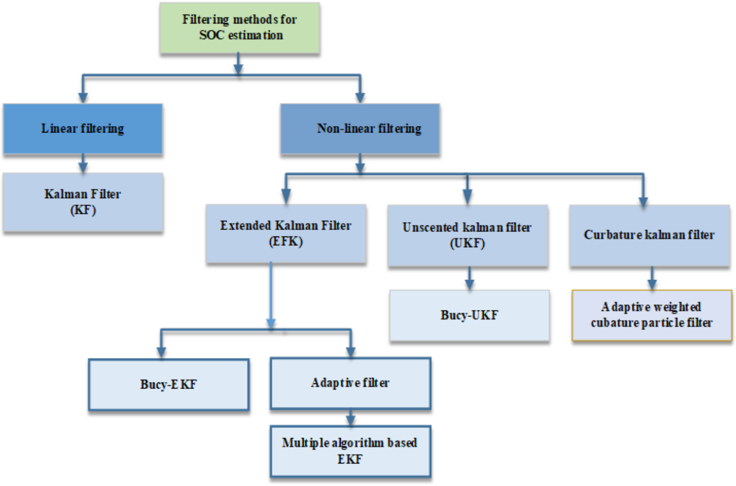

Figure 2.9: Filtering Method Categories

2.5.1 The Kalman Filter: A Two-Step Process

Figure 2.10 [48] demonstrates how the Kalman filter continuously refines SOC estimates through its dual-phase operation

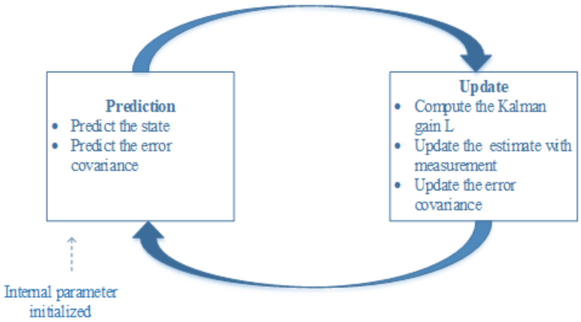

:

Figure 2.10: Iterative prediction-correction cycle of the Kalman filter.

This method combines the best of both worlds: a battery model *and* real-time observation. The Kalman filter acts like a smart interpreter, using live battery data (voltage and current measurements from the equivalent circuit model) as its starting point to continuously refine its predictions

Integrated SOC Estimation Framework

1A step: Time update for state prediction

$$\hat{a}_k^- = E[a_k|Y_{k-1}] = E[f(a_{k-1}, c_{k-1}, e_{k-1})|Y_{k-1}] \qquad (5)$$

1B step: Time update for error covariance

$$\Sigma_{\tilde{a},k}^- = E[(\tilde{a}_{\bar{k}})(\tilde{a}_{\bar{k}})^T] = E[(a_k - \hat{a}_{\bar{k}})(a_k - \hat{a}_{\bar{k}})^T] \qquad (6)$$

1C step: A system's output estimation$\hat{b} = E[b_k|Y_{k-1}] = E[h(a, c_k, d_k)|Y_{k-1}]$ (7)

2A step: Gain matrix for estimator

$$G_k = \Sigma_{\tilde{a}\tilde{b},k}^- \Sigma_{\tilde{b},k}^- 1 \qquad (8)$$

2B step: Update the state estimation measurement

$$\hat{a}_k^+ = \hat{a}_k^- + G_k(b_k - \hat{b}_k) \qquad (9)$$

2C step: Update the error covariance measurement.

$$\Sigma_{\tilde{a},k}^+ = \Sigma_{\tilde{a},k}^- - G_k \Sigma_{\tilde{b},k}^- G_k^T \qquad (10)$$

For nonlinear systems (common in real-world batteries), EKF/UKF variants overcome linearity limitations while retaining this recursive structure. Assumptions: system/observation noise vectors (w,v) have zero mean.

2.5.2 Extended Kalman Filter

The extended Kalman Filter is one of the most useful algorithms for nonlinear filter systems to offer real-time SOC estimation **[49]**. EKF's basic idea is to focus on the significance of first-order nonlinear Tylor series expansion **[50]** with respect to the estimation state. EKF then linearizes the nonlinear system by converting it into a linear equation **[51]**. EKF is used to estimate the best and most accurate SOC values. To find the terminal voltage and current values, SOC estimation uses ECM as an input or as a starting point. In **Figure 2.11**, the EKF algorithm is presented.

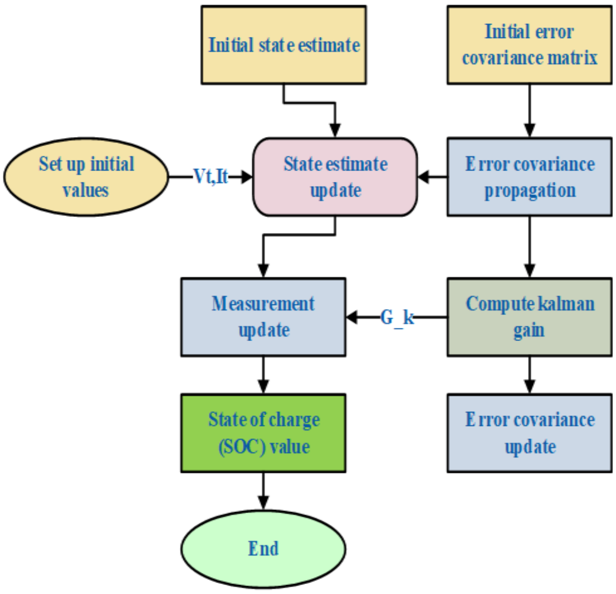

Figure 2.11: The Extended Kalman filter algorithm

Evaluating the subsequent EKF equations

EKF 1A step: During time updates, the EKF predicts future states via:

$\hat{a}_k^- = E[f(a_{k-1}, c_{k-1}, e_{k-1})|Y_{k-1}]$ (11)

Where $\bar{e}_{k-1} = E[e_{k-1}]. (\text{Often}, e_{k-1} = 0.)$ (12)

$e_{k-1} = 0$

$\hat{a}_{k-1}^+$ & $\bar{e}_{k-1}$ are assumed to be logically propagable by the state equation, resulting in the expected value of the new state.

EKF 1B step: Time update for error covariance

Making an approximate calculation for $\tilde{a}_{\bar{k}}$ is the first stage in the covariance prediction process.

$\tilde{a}_{\bar{k}} = a - \hat{a}_{\bar{k}}$ (13)

$= f(a_{k-1}, c_{k-1}, e_{k-1}) - f\,f(\hat{a}_{k-1,}^+ c_{k-1}, \bar{e}_{k-1}).$ (14)

EKF 1C step: System's output estimation

The estimated system output is

$\hat{b}_k = E[h(a_k, c_k, d_k)|Y_{k-1}]$ (15)

$\approx h(\hat{a}_{k-1,}^- c_k, \bar{d}_k),$

It is therefore assumed that the mean sensor noise and $\tilde{a}_{\bar{k}}$ are the best approximations for calculating the output.

EKF 2A step: Estimators' gain matrix

$\tilde{b}_{\bar{k}} = b_k - \hat{b}_{\bar{k}} = h(a_k, c_k, d_k) - h(\hat{a}_{k-1,}^- c_k, \bar{d}_k)$ (16)

EKF 2B step: Update the state estimation measurement

In this stage, the prediction is updated using the estimator gain, and the innovation $b_k - \hat{b}_{\bar{k}}$ provides the posterior state estimate.

$\hat{a}_k^+ = \hat{a}_k^- + G_k(b_k - \hat{b}_{\bar{k}})$ (17)

EKF 2C step: Update measurement of the error covariance

$\sum_{\hat{a},k}^{+} = \sum_{\hat{a},k}^{-} - G_k \sum_{\hat{b},k}^{-} G_k^T$

2.5.3 Advanced Estimation with Unscented Kalman Filtering

While EKF struggles with computational complexity from its linearized Taylor approximations **[52]**, the Unscented Kalman Filter (UKF) offers smarter nonlinear estimation. Instead of linearizing, UKF strategically samples 'sigma points' shown in **Figure 2.12** to capture true system behavior with 2nd-order accuracy **[53-56]**—yielding more reliable SOC predictions through its sampling mean (a) and covariance (G) adjustments.

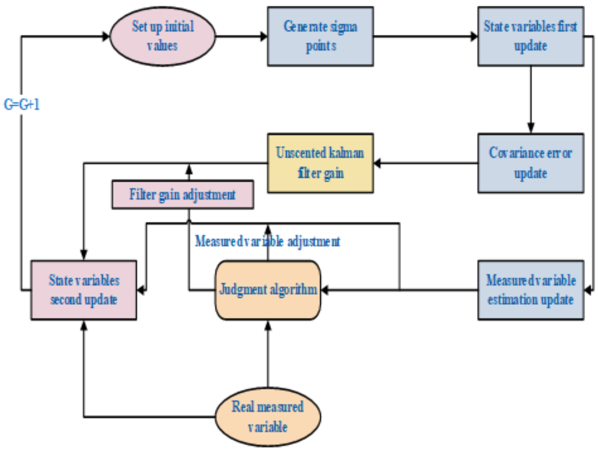

Figure 2.12: The algorithm for unscented Kalman Filter

UPKF 1A step: Time update for state prediction
Start by creating a posteriori state estimate vector for the previous time interval:
$\hat{a}_{k-1}^{x,+} = (\hat{a}_{k-1}^{+})^T, \bar{e}, \bar{d}]^T$ (19)

And enhanced a posteriori covariance estimation:
$\sum_{\hat{a},k}^{x,+} = \text{Diag}\,(\sum_{\hat{a},k}^{+} \sum \tilde{e}, \sum \tilde{d})$ (20)

To produce the p+1 augmented sigma points, these variables are used.
$R_{k-1}^{x,+} = \{\hat{a}_{k-1}^{x,+}, \hat{a}_{k-1}^{x,+} + \beta\sqrt{\sum_{\hat{a},k-1}^{+}}, \hat{a}_{k-1}^{x,+} - \beta\sqrt{\sum_{\hat{a},k-1}^{+}}.\}$ (21)

SPKF 1B step: Time update for error covariance
$\sum_{\bar{a}k}^{-} = \sum_{i=0}^{p} \alpha_i{}^{(c)} (R_{k,i}^{x,-} - \hat{a}_{\bar{k}})(R_{k,i}^{x,-} - \hat{a}_{\bar{k}})^T$ (22)

SPKF 1C step: System's output estimation b_k
The output b is estimated by assessing the model's final equation
Firstly we calculate the points.
$b_{k,i} = h(R_{k,i}^{a,-}, u_k, R_{k-1,i}^{a,+})$ (23)
Next, the output estimation is
$\hat{b}_k = E[b(a_k, c_k, d_k)|Y_{k-1}]$ (23)
$\approx \sum_{i=0}^{p} x_i{}^{(m)} \left(R_{k,i}^{x,-}, c_k, R_{k-1,i}^{x,+}\right)$ (24)
$= \sum_{i=0}^{p} x_i{}^{(m)}\, b_{k,i}$ (25)
As we did when determining $\hat{a}_k^-$ after the 1A step, this can be calculated using straightforward matrix multiplication.
SPKF 2A step: Gain matrix for estimators G_k.
$\sum_{\hat{b},k} = \sum_{i=0}^{p} x_i{}^{(c)} (b_{k,i} - \hat{b}_k)(b_{k,i} - \hat{b}_k)^T$ (26)
$\sum_{\bar{a},\bar{b}k}^{-} = \sum_{i=0}^{p} x_i{}^{(c)} (R_{k,i}^{x,-} - \hat{a}_{\bar{k}})(R_{k,i}^{x,-} - \hat{b}_{\bar{k}})^T$ (27)

Both of these are dependent on the sigma-point matrices R and b_k, which were already computed in steps 1B and 1C, as well as $\hat{a}_k^-$and $\hat{b}_k$, which were already computed in the above steps.
Matrix multiplies can be used to produce the summing, as we did in the 1B step.
Next, we just compute.

$$G_k = \Sigma^-_{\tilde{a}\tilde{b},k}\Sigma^-_{\tilde{b},k} 1 \quad (28)$$

SPKF 2B step: Update the state estimation measurement
The calculation for the state estimate is

$$a_k^+ = \hat{a}_k^- + G_k(b_k - \hat{b}_{\bar{k}}) \quad (29)$$

SPKF 2C step: Update for error covariance
The optimal formulation is utilized to calculate the final step directly.

$$\Sigma^+_{\tilde{a},k} = \Sigma^-_{\tilde{a},k} - G_k \Sigma^-_{\tilde{b},k} G_k^T \quad (30)$$

2.5.4 Adaptive Filters

Adaptive filters offer a dynamic solution for SOC estimation by continuously adjusting to battery aging and operational changes, overcoming limitations of static models. The Recursive Least Squares (RLS) algorithm **[57]** excels in real-time system identification, providing fast convergence for ECM parameter estimation, while adaptive EKF variants **[58]** enhance noise tracking capabilities. For simpler implementations, the Least Mean Squares (LMS) approach **[59]** operates reliably with incomplete data streams, though its susceptibility to weight drift has spurred specialized variants like Polarity-Based and Self-Adjusting Step Size LMS. Particle filters complement these methods by handling severe nonlinearities through probabilistic sampling. Together, these adaptive techniques provide robust SOC estimation across a battery's operational lifespan by addressing the inherent nonlinearities and time-varying characteristics of lithium-ion cells **[60]**

2.6 Data-Driven Estimation Methods

A branch of machine learning that focuses on multi-layered artificial intelligence networks is the trained data estimation approach. This approach, which has been shown to be reliable and effective, estimates the SOC**.**

2.6.1 Feed-Forward Neural Network

In a feedforward neural network, data is sent from source to sink in a single direction without iterations or intervals. Another term for this particular kind of neural network is the multilayer perceptron (MLP). In a neural network, data travels via intermediate hidden layers from the first layer to the final layer predictions or classifications **[61–62]**. The FNN uses a variety of input characteristics, including temperature, time, voltage, and current, to predict the state of charge. In this study, the network method is shown in **Figure 2.13**.

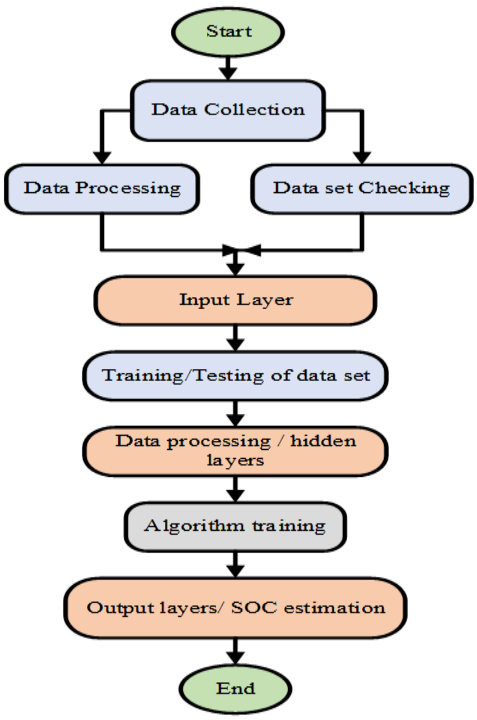

Figure 2.13: SOC estimate using FNN

III. METHODOLOGY

3.1 Model-based Estimation Method

In order to avoid adverse impacts on battery characteristics, ECM is frequently utilised as a simple parameter identification. In addition to analysing voltage and current behaviour, this model is used to determine key battery parameters such internal impedance, resistance, and charge status. These projections help manage and monitor batteries for electric vehicles. Better outcomes, more accuracy, and less complexity follow.

3.1.1 2nd Order RC ECM

In comparable circuit modeling, a second-order RC model is frequently used to depict the properties of Li-ion batteries. The battery is represented in this model by a parallel connection of resistors (r1, r2) and capacitors (c1, c2). Capacitors, resistors, and voltage sources make up an analogous circuit model. Temperature T, battery state of charge (SOC), charging current (Ic), and terminal voltage (Vt) will all be measured by the ECM. A simple ECM with an ohmic resistor Ro and a voltage source as seen in **Figure 3.1**. MATLAB is used to build a second order RC circuit design with preset variables.

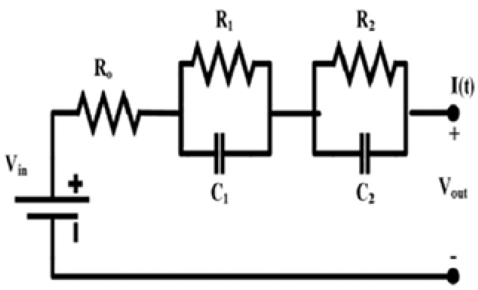

Figure 3.1: 2nd Order RC ECM schematic Layout.

3.1.2 Filtering Procedure

Inner parameter values that serve as initializations in the SOC estimate process are determined by the Equivalent Circuit Model (ECM). It will be suggested that the Kalman, Extended, and Unscented filters be utilized. **Figure 3.2** explains the state and update equation step technique.

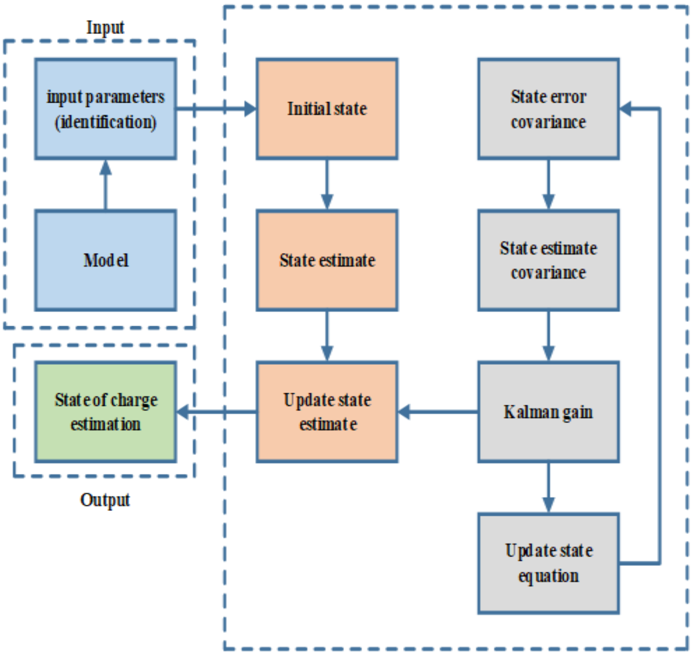

Figure 3.2: Kalman filtering state and update procedure based on ECM

3.1.3 State Transition Diagram

Figure 3.3 presents the state transition algorithm for lithium-ion battery SOC/SOH estimation across three operational modes. During charging, voltage increases until threshold, while current (Ib) drops sharply then gradually to zero at full charge, enabling SOC derivation from constant-current charging curves. In discharge mode, voltage-current correlation allows SOC calculation through current variation analysis, transitioning to OCV-based reference during inactive periods. Our three-stage approach first establishes ECM baseline parameters, then applies Kalman filters for SOC estimation, and finally employs UKF for enhanced dynamic condition accuracy. The UKF-based health monitoring system integrates real-time voltage, current and temperature data to evaluate remaining capacity (%), performance efficiency and reliability - critical metrics for EV battery management.

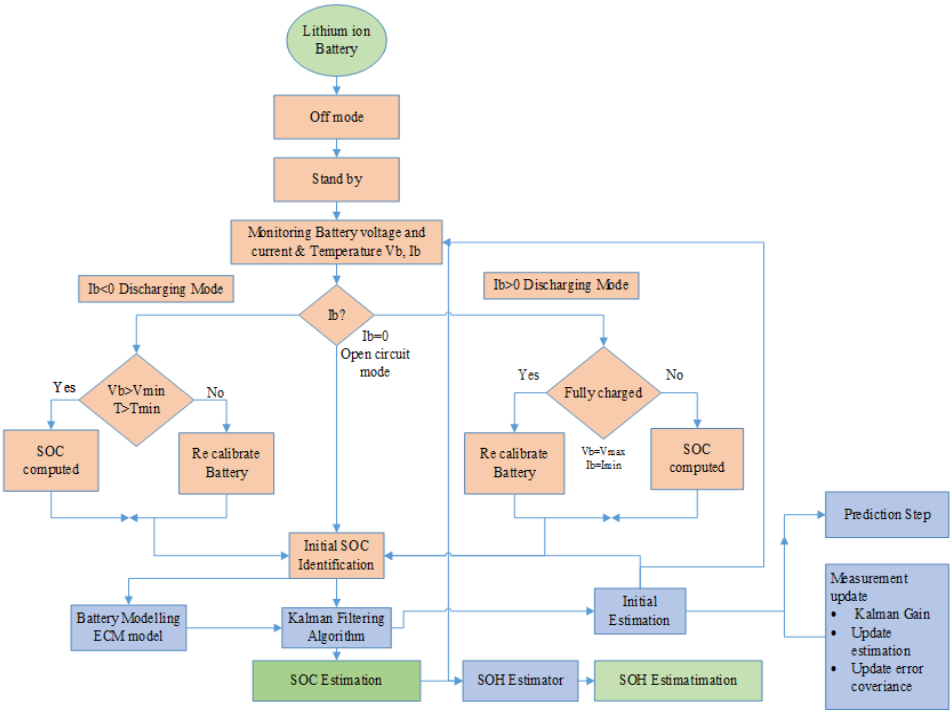

Figure 3.3: SOC & SOH state transition flowchart for lithium-ion battery

3.1 Trained Data Estimation Method

A train data-based FNN framework for SOC estimation was presented in this part. The battery data is necessary in order to train the FNN. Data about temperature, average current, average voltage, and voltage must be gathered. Following the collection of parameters, the layer data will be required.

3.1.1 Data Acquisition

As was already indicated, **Figure 3.4** illustrates the three levels of FNN. The input layer is a design's initial layer. Temperature, average current, voltage, and current have all been measured in order to train the initial layer of design. The second hidden layer is where the first data is processed. For our proposed approach, we generated 55 neurons in this layer. The last layer is the output layer, which combines the input and hidden layers.

3.1.2 Data Computation

The process of compiling all the data required to finish an operation into a single unit is known as data computation. The next step determines the length of a sequence and small batch measurements to ensure consistency throughout the dataset. There should be no difference between the test and validation data sets.

3.1.3 Designing Networks

As shown in **Table 4**, we supplied the network architecture with the necessary FNN variables. The iteration level should be at least 20 for accuracy. Small batches and training capacities determine how accurate the validation data is. In order to obtain more precise and useful findings in our case, we completed the initial data processing without rearranging the data. The process diagram of FNN is shown in **Figure 3.5.**

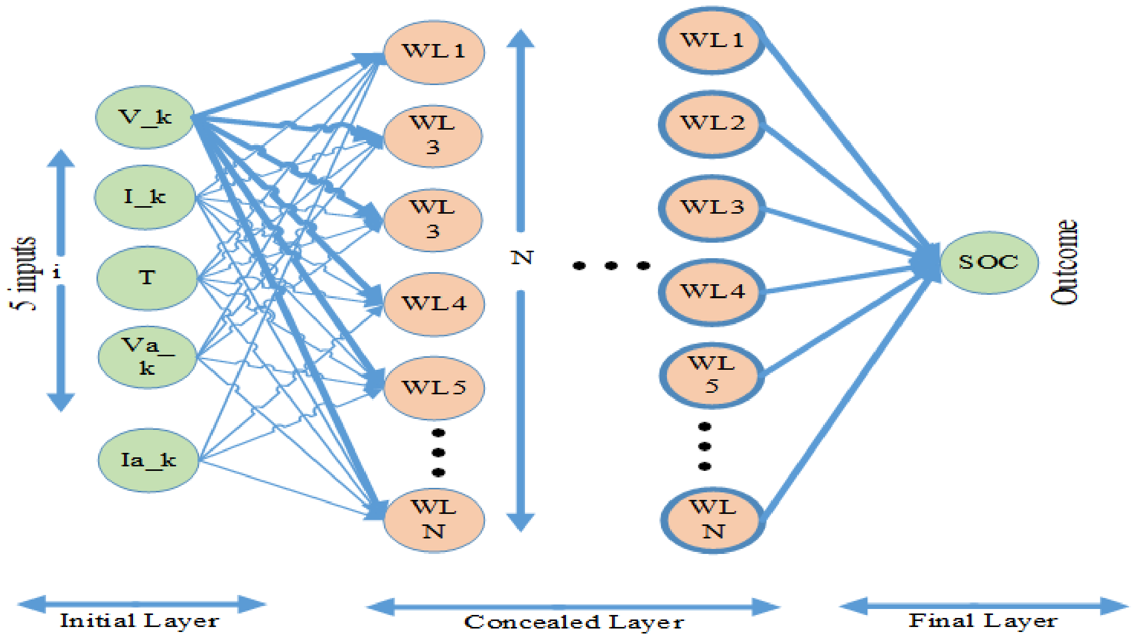

Figure 3.4: FNN layering diagram

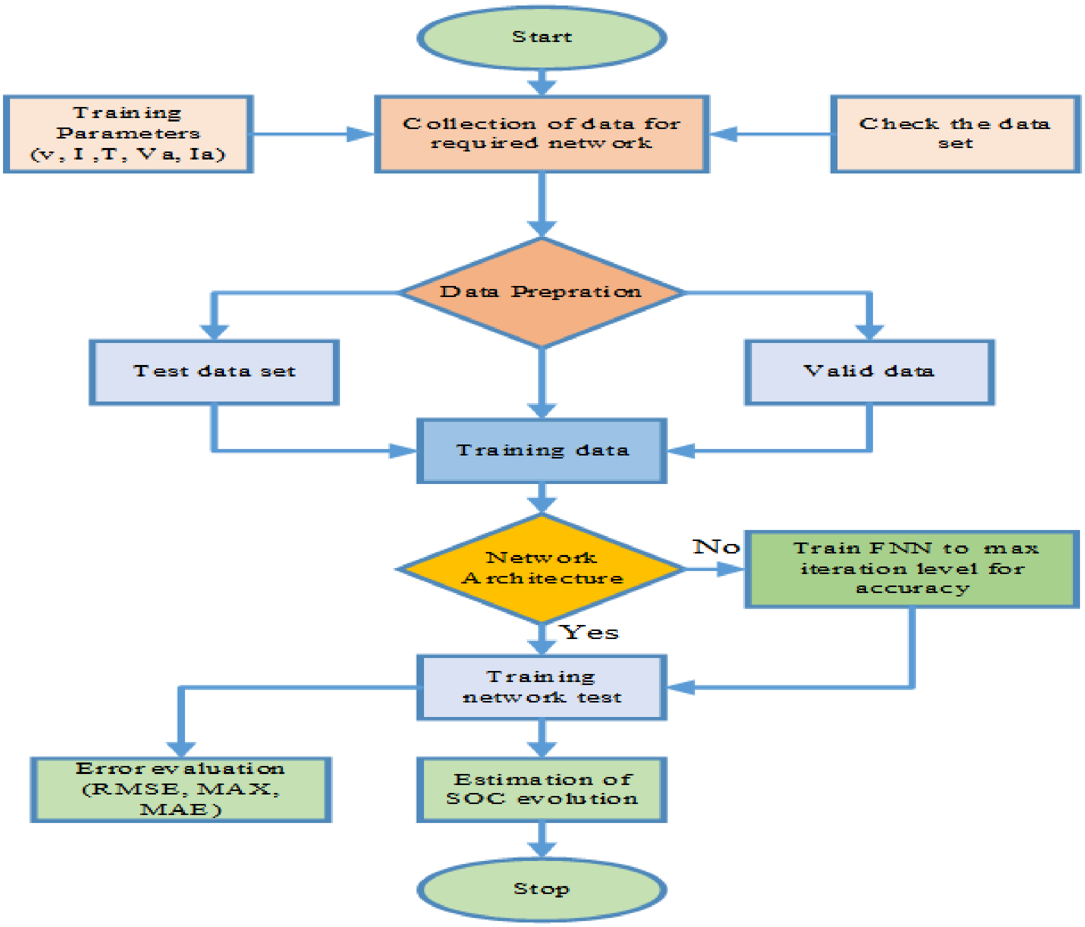

Figure 3.5: Train data estimation network's flow diagram

IV. Experiments and Results

4.1 How We Estimated Battery States

Our experiments followed the SOC estimation process shown in **Figure 3.3**. Here's what we found:

4.1.1 Measuring Battery Characteristics

We built a 2RC equivalent circuit model in Simulink (**Figure 4.1**) to pin down the lithium-ion battery's exact parameters. This model helps us understand how the battery behaves in different conditions. The subsystem of 2RC cell is shown in **Figure 4.2**.

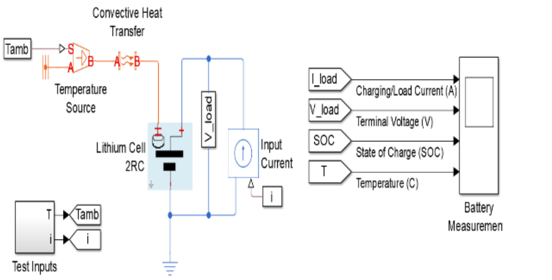

Figure 4.1: Simulink implementation of the 2RC circuit model for battery parameterization.

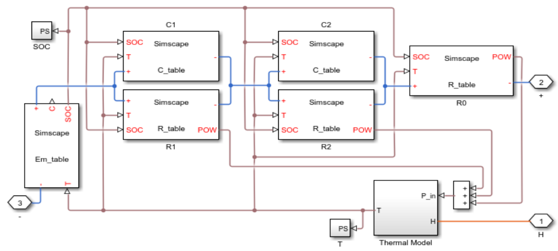

Figure 4.2: Subsystem for 2-RC Lithium Cell equivalent

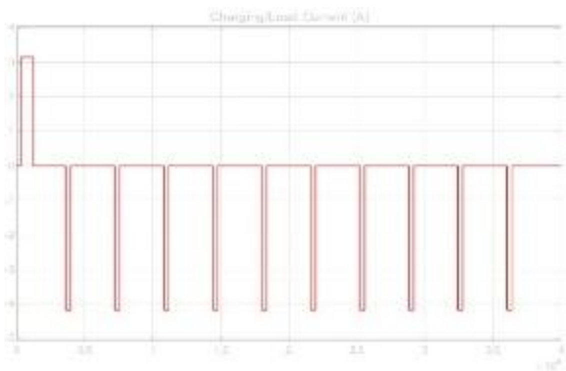

Figure 4.3: Charging Current

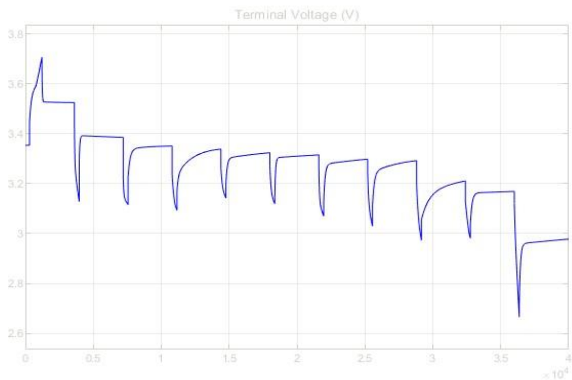

Figure 4.4 Terminal Volt

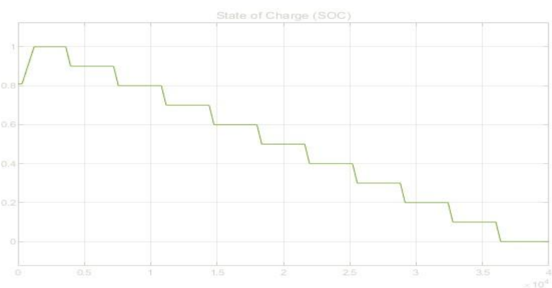

Figure 4.5: State of charge

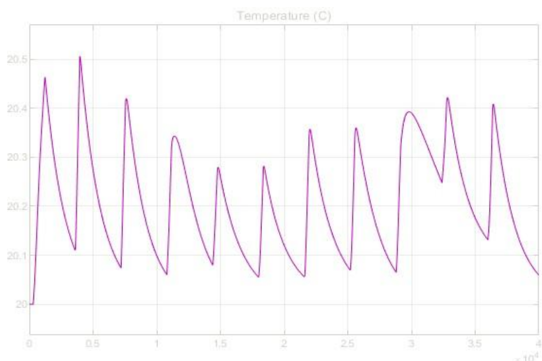

Figure 4.6: Temperature

We analyze battery performance using a hybrid pulse discharge method, initialized at 100% SOC to track parameter changes. During testing, the lithium-ion battery undergoes repeated charge/discharge cycles, generating pulse-form data for each phase. The 2RC equivalent circuit model proves superior to the 1RC alternative, offering greater accuracy in capturing complex battery dynamics—including external voltage behavior and internal parameter shifts. Key results (**Figures 4.3–4.6**) depict load current, terminal voltage, temperature fluctuations, and SOC trends, revealing predictable capacity fade with cycling. Initial SOC values typically range from 80–100%, with a stable 'flat zone' near 80% SOC followed by a gradual rise during charging. Derived 2RC parameters are summarized in **Table 2**.

Table 2: Identified Parameters of the 2-RC Equivalent Circuit Model

Parameters	Range
V_t Voltage Range	3.3 - 3.7 V
I_L Current Flow	Alternates between -4.2A (discharging) and +3.2A (charging) in intermittent bursts
T(Operating Temperature)	-20~20.1 ºC
SOC (**Initial** state of charge)	80~100% then progressively decline after each period

The mathematical framework is set up in KF, EKF, and with inputs obtained from the battery design in order to estimate SOC.

4.1.2 Results of the Filtering Process

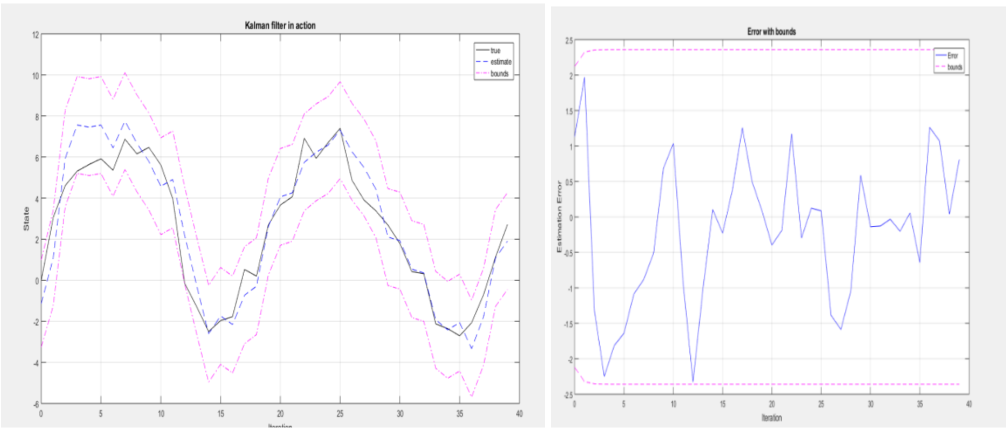

Figure 4.7: Kalman filter (i) True, estimated, & bound results (ii) Error of SOC estimation

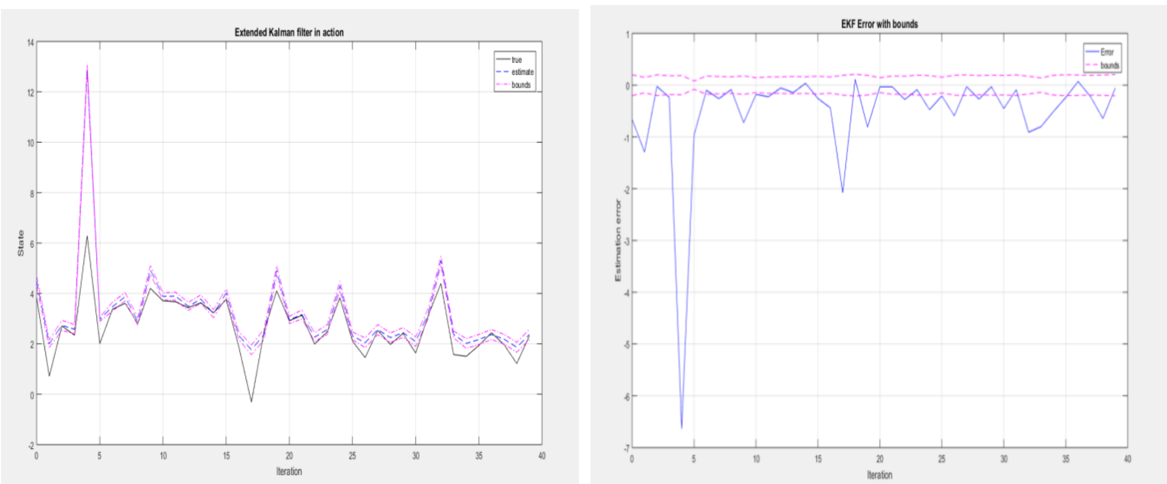

Figure 4.8: Extended Kalman Filter (i) True, estimated, & bound results (ii) Error of SOC estimation

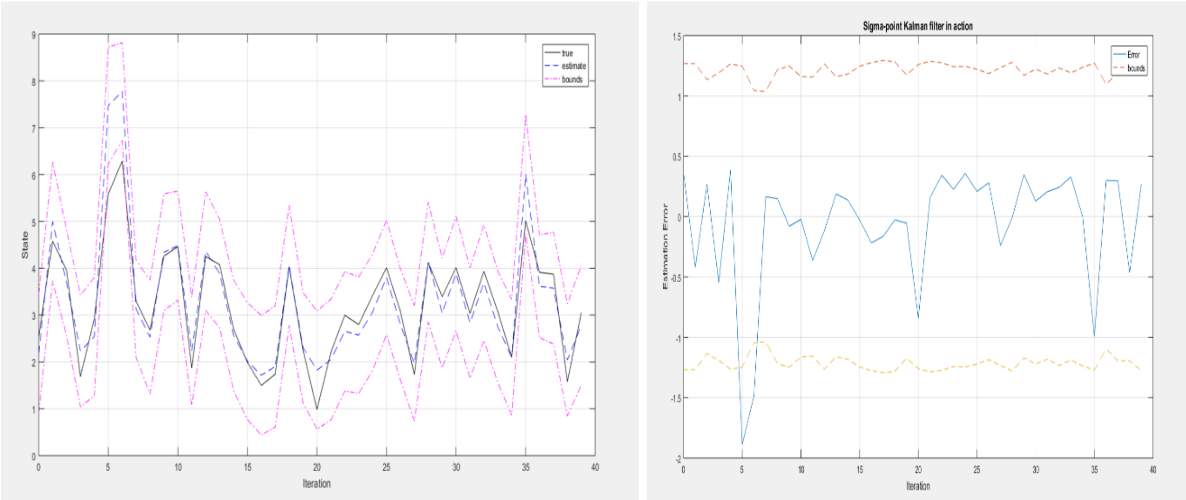

Figure 4.9: Unscented Kalman Filter Performance
(i) True state, estimated state, and confidence bounds
(ii) State of Charge (SOC) estimation error

Table 3 Error Analysis of the Filtering Method

Error	KF	EKF	UKF
Error at bounds	± 2.4	± 2	± 1.4
Error of estimation	< 1.6	< 0.6	< 0.4

To get reliable SOC estimates, we start by zeroing out the detector (d_k) and process noise (e_k), then let the Kalman filter work under real-world noisy conditions. When we compare methods (**Figs. 4.7-4.9**), the UKF stands out—it locks onto the true SOC faster than traditional KF or EKF, cutting errors to under 0.4% thanks to its clever sigma-point sampling. This isn't just theory: the UKF's precision (**Figure 4.10)** shows a razor-thin 0.01% SOH error) actually translates to better EV performance and longer battery life listed in **Table 3**.

4.1.2 Unscented Kalman Filter SOC & SOH Estimation

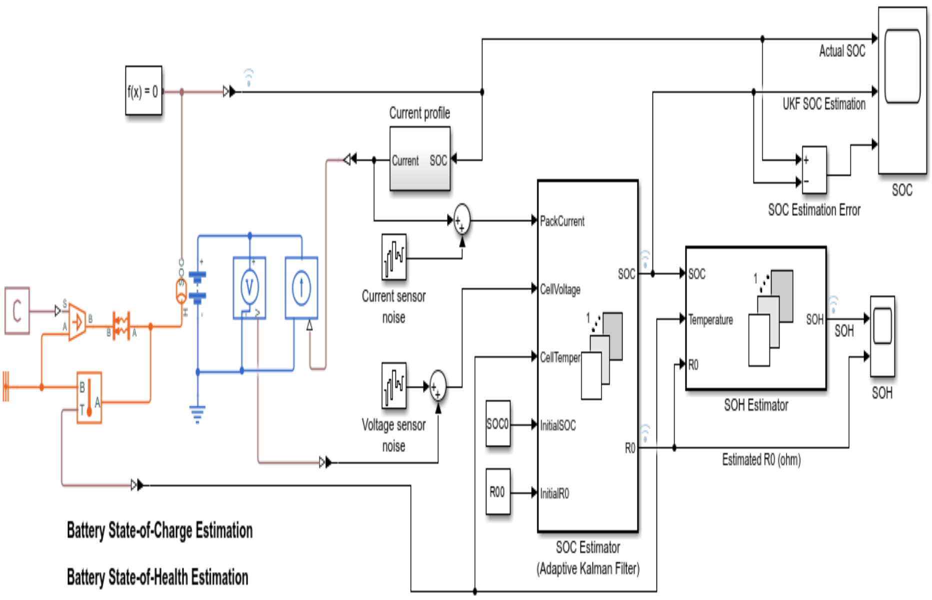

(i)

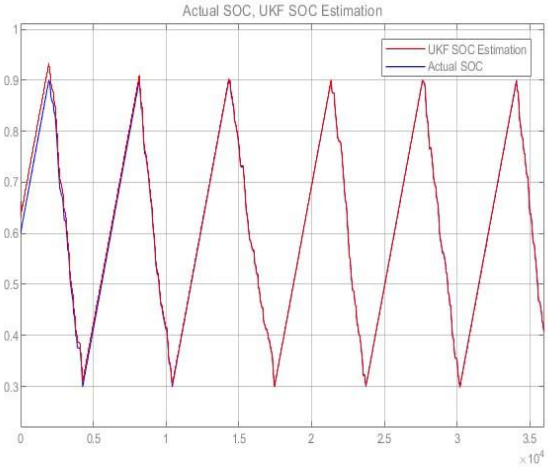

(ii)

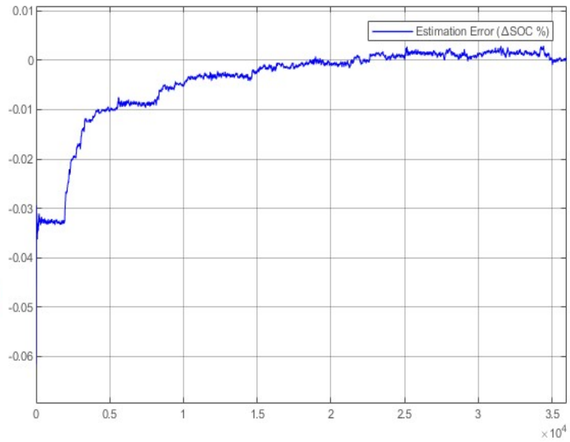

(iii)

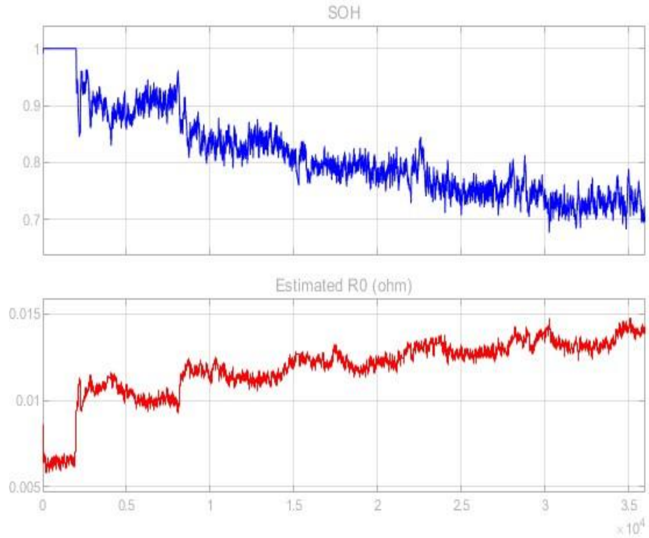

(iv)

Figure 4.10: Performance of the Unscented Kalman Filter (UKF) for (i) Battery State Estimation (ii) Real value vs. estimated value (iii) Estimation error (iv) State of health and estimated resistance

4.1 Train Data Estimation Method

This chapter presents the Root Mean Square Error (RMSE), Maximum Error (MAX), and Mean Absolute Error (MAE) for State of Charge (SOC) estimation, following the FNN process outlined in **Figure 3.5** and the network specifications detailed in **Table 4**. The training process was repeated three times, with the results summarized in **Tables 5 to 7**. These experiments used the Adaptive Moment Estimation (ADAM) optimizer, running for 200 epochs with validation performed every 30 iterations.

The initial RMSE results from the computational analysis are illustrated in **Figures 4.11 to 4.13**, while **Figures 4.14 to 4.20** display the RMSE, MAX, and MAE errors at different temperatures (–10°C, 0°C, 10°C, and 25°C). To train the FNN for SOC prediction, input variables such as voltage, current, average current, average voltage, and temperature were collected at each time step. Before training, the data underwent pre-processing to ensure proper validation, testing, and network training. Analysis at different temperatures is listed in **Table 8**. Comparative analysis of evolving variables and operating characteristics is presented in **Table 9**.

Table 4: Key Architectural and Training Parameters for the Feedforward Neural Network (FNN)

Parameters	Given data
Number of output neurons	1
Number of input features	5
Total neurons in hidden layers	55

Training epochs	200
Epochs required for learning rate decay	1000
Initial learning rate	0.01
Learning rate decay factor	0.1
Validation frequency (epochs)	30
Training repetitions	3

4.2.1 Input Data Normalization Protocol

Table 5: First Repetition Performance Metrics

Epoch	Iteration	Time Elapsed (hh:mm:ss)	Mini-batch RMSE	Validation RMSE	Mini-batch Loss	Validation Loss	Base Learning Rate
1	1	00:00:09	0.70	0.38	0.2477	0.0711	0.0100
30	30	00:02:01	0.05	0.07	0.0012	0.0022	0.0100
50	50	00:03:18	0.03		0.0006		0.0100
60	60	00:03:56	0.03	0.03	0.0006	0.0003	0.0100
90	90	00:05:51	0.03	0.03	0.0005	0.0003	0.0100
100	100	00:06:30	0.03		0.0005		0.0100
120	120	00:07:46	0.03	0.02	0.0005	0.0003	0.0100
150	150	00:09:43	0.03	0.03	0.0004	0.0006	0.0100
180	180	00:11:51	0.03	0.02	0.0004	0.0002	0.0100
200	200	00:13:15	0.03	0.02	0.0004	0.0002	0.0100

Table 6: Third Repeat

Epoch	Iteration	Time Elapsed (hh:mm:ss)	Mini-batch RMSE	Validation RMSE	Mini-batch Loss	Validation Loss	Base Learning Rate
1	1	00:00:08	0.69	0.45	0.2393	0.1013	0.0100
30	30	00:01:53	0.05	0.06	0.0013	0.0019	0.0100
50	50	00:03:11	0.04		0.0007		0.0100
60	60	00:03:53	0.04	0.04	0.0006	0.0007	0.0100
90	90	00:05:54	0.03	0.05	0.0005	0.0010	0.0100
100	100	00:06:34	0.04		0.0006		0.0100
120	120	00:07:55	0.04	0.04	0.0006	0.0006	0.0100
150	150	00:09:46	0.03	0.04	0.0005	0.0006	0.0100
180	180	00:11:43	0.03	0.03	0.0005	0.0004	0.0100
200	200	00:13:00	0.03	0.03	0.0004	0.0005	0.0100

Table 7: Model Robustness Analysis Across Repeated Validations

Repetition no.	Validation RMSE %	Validation Loss
1	0.02	0.0002
2	0.03	0.0005
3	0.03	0.0005

4.2.2 Training & Validation Performance Analysis

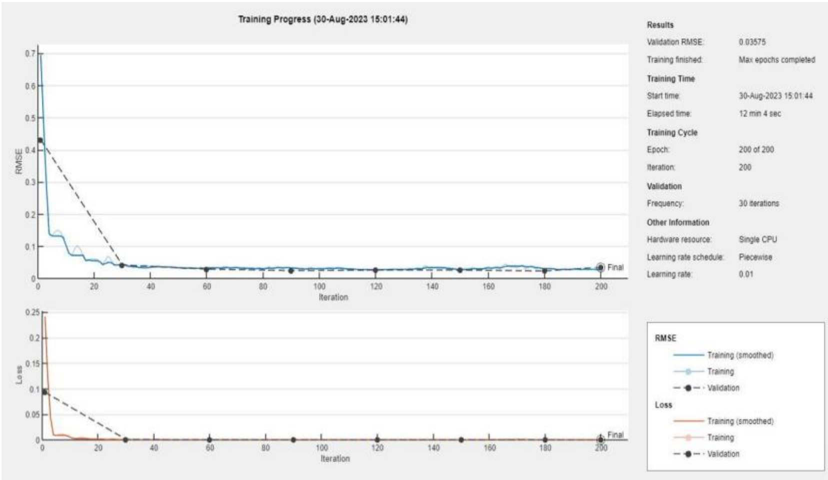

Figure 4.11: First repeat

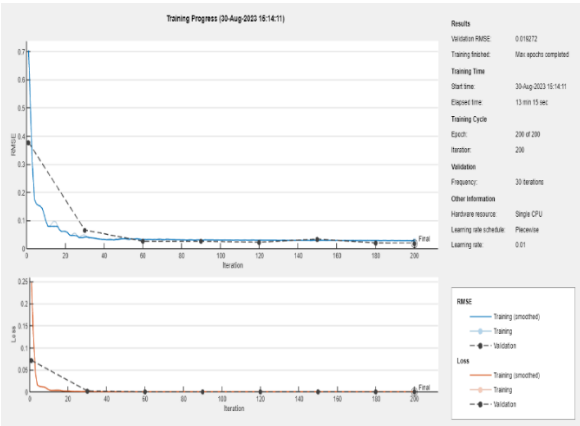

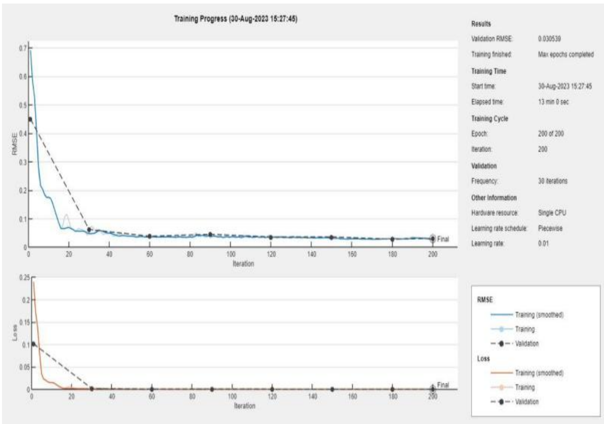

Figure 4.12: Second repeat **Figure 4.13: Third Repetition Performance Benchmark**

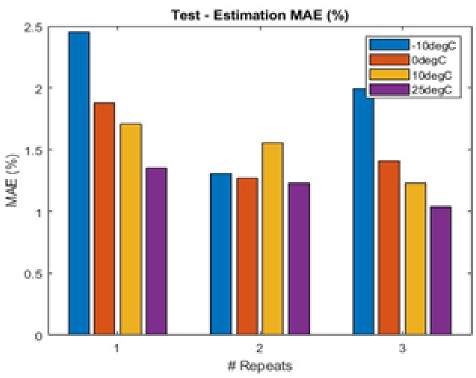

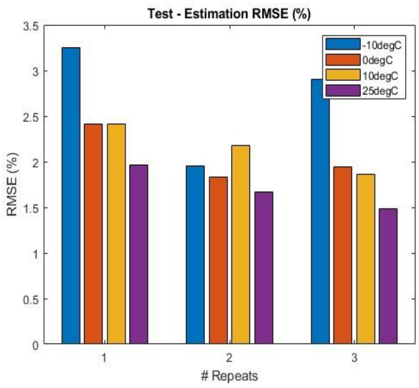

Figure 4.14 **Figure 4.15**

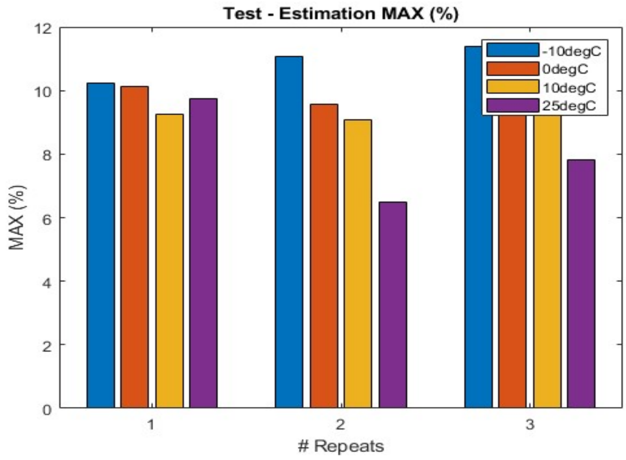

4.16: Estimation Error Stability Analysis

Table 8: Comparative Analysis of Estimation Methods for Dynamic Systems

Repeat stage no	RMSE (%)	MAE (%)	MAX (%)
1. Subzero Performance (-10°C)			
1	0.033	0.024	0.100
2	0.02	0.013	0.110
3	0.029	0.013	0.115
2. Freezing Point (0°C)			
1	0.024	0.019	0.100
2	0.019	0.012	0.097
3	0.02	0.012	0.105
3. Cool Conditions (10°C)			
1	0.024	0.017	0.095
2	0.022	0.016	0.095
3	0.019	0.013	0.100
4. Room Temperature (25°C)			
1	0.019	0.013	0.098
2	0.016	0.012	0.065
3	0.015	0.01	0.079

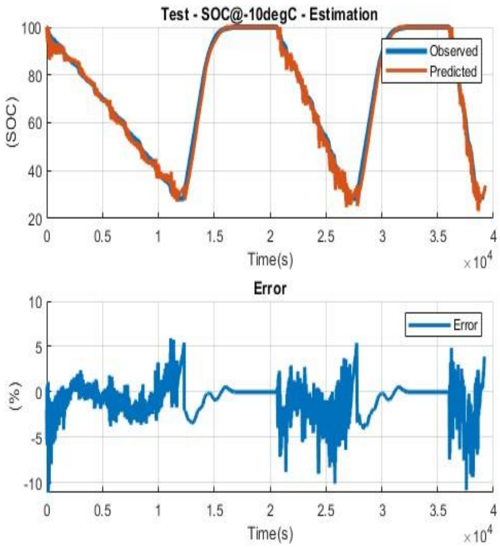

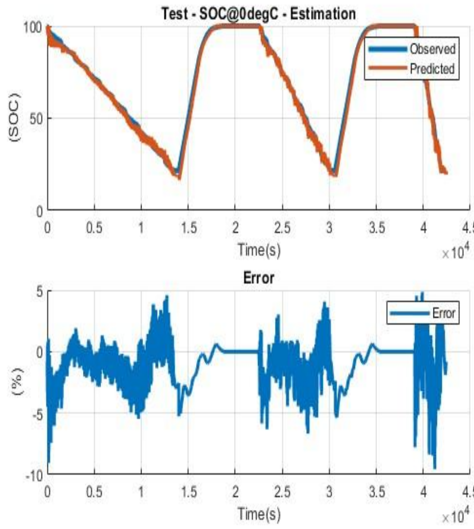

Figure 4.17: Test at (-10°C)   Figure 4.18: Test at (0°)

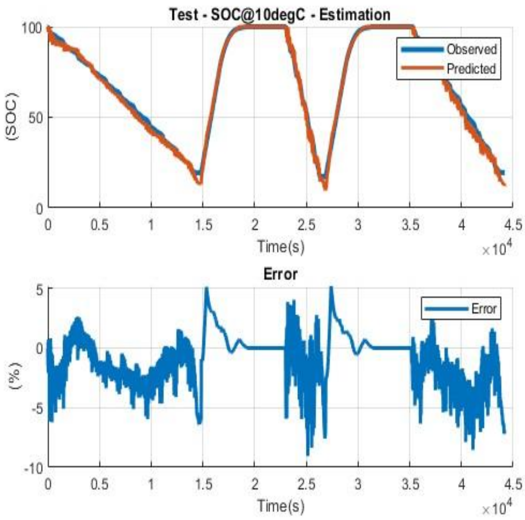

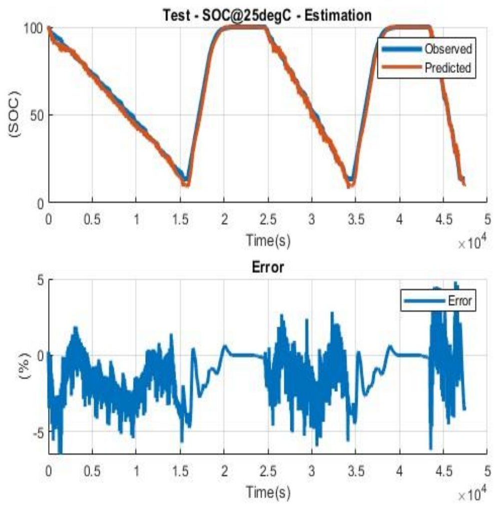

Figure 4.19: Room-Temperature (10°C) Estimation Benchmark Figure 4.20: Moderate Temperature Performance (25°C)

Table 9: Comparative Analysis of Evolving variables and Operating characteristics

Sr.no	Estimation Technique	Core Methodology	Evolving variables				Operating characteristics		
			E1	E2	E3	E4	O1	O2	O3
			Accuracy (RMSE)	Processing Time	Design Constraints	Recovery Capability	System Efficiency	SOC Error (%)	Predictive Utility
1	Feed-forward neural network	Layered artificial neuron architecture	Exceptional (<0.02%)	Moderate	Significant limitations	Outstanding	Optimal	(< 0.02)	Adaptive value prediction
2	Unscented Kalman filter	Deterministic sampling for nonlinear systems	Outstanding (<0.01%)	High latency	Minimal constraints	Outstanding	Optimal	(< 0.01)	Degradation pattern analysis
4	Extended Kalman filter	First-order linearization approximation	Competitive (<0.6%)	Efficient	Moderate constraints	Outstanding	Optimal	(< 0.6)	Remaining useful life projection
5	Kalman filter	Linear system state estimation	Acceptable (<2%)	Moderate	Significant constraints	Limited	Optimal	(< 2)	Real-time state tracking
6	Coulomb Counting	Current-time integration method	Tolerable (<2.7%)	Rapid	Significant constraints	Limited	Suboptimal	(< 2.7)	Historical data dependence

V. Conclusion

It is advised that lithium-ion batteries be used in cars using the SOC estimate method. MATLAB simulations for various stages of lithium-ion battery degeneration have been used to validate them. The results show that the KF, EKF, and UKF-based ECM's estimated errors are contained within a restricted range. Although UKF and EKF both perform well, UKF's error reduction is ±0.035% when compared to EKF and ±1.6% when compared to KF. This highlights the UKF's crucial function in SOC estimation because it successfully lowers the estimated RMSE to 0.01. A narrow range of errors indicates that these methods may eliminate noisy measurements and operational errors, ensuring accurate SOC convergence under time-dependent estimate errors.

But when compared to all of the above techniques, the training data approach, FNN, shows noticeably lower estimation errors. Since they successfully lower system noise and guarantee the safe functioning of EVs, both strategies have undergone extensive verification and are considered appropriate for EVs.

Research on SOC estimate has made significant strides, but a solid methodology to overcome the shortcomings of previous methods has not yet been developed. This study demonstrates the superior outcomes of the suggested methods for estimating SOC, specifically the UKF in conjunction with ECM. These model-based filtering strategies show improved precision, more adaptability, and reduced prediction error compared to previous filtering techniques. Additionally, the article proposes a revolutionary technology known as Feed Forward Neural Network (FNN), which blends prediction techniques with artificial intelligence to produce extremely dependable results. FNN accelerates the rate of learning for SOC estimation by outperforming recently proposed techniques in terms of lowest RMSE, MAE, and MAX errors. Similarly, this paper presents a technique for accurate SOC estimation using FNN under different temperature settings. The literature hasn't before examined this strategy. The proposed method is less complex and more adaptable since it may effectively train any pertinent operation with the right datasets. The findings demonstrate that, in comparison to traditional approaches, both of the proposed methods provide correct SOC estimations with short computation times, demonstrating exceptional precision and rapid convergence.

REFERENCES

[1] I. Arasaratnam, “Novel Battery SOC/SOP/SOH Estimation Algorithms in a Unified Framework.”

[2] D. Panigrahi, C. Chiasserini, S. Dey, and R. Rao, “Battery Life Estimation of Mobile Embedded Systems 2 Motivation : Exploration For Bat- tery Efficient Architectures,” *Proc. Fourteenth Int. Conf. VLSI Des.*, pp. 57–63, 2001.

[3] J. P. Salameh, N. El Ghossein, M. El Hassan, N. Karami, and M. B. Najjar, “Battery Modeling and Lifetime Prediction,” *Mod. Environ. Sci. Eng.*, vol. 04, no. 03, pp. 278–290, 2017, doi: 10.15341/mese(2333-2581)/04.03.2017/008.

[4] “Lithium- İon battery charging and discharging monitoring system (BMS) based on Stm32,” vol. 7, no. 3, pp. 10–15, 2019.

[5] M. Murnane and A. Ghazel, “A Closer Look at State of Charge (SOC) and State of Health (SOH) Estimation Techniques for Batteries,” *Analog devices*, 2017.

[6] F. S. Barnes and I. Scott, “Battery Energy Storage,” *Large Energy Storage Syst. Handb.*, pp. 160–186, 2018, doi: 10.1201/b10778-10.

[7] J. P. Nelson and W. D. Bolin, “Basics and Advances in Battery Systems,” *IEEE Trans. Ind. Appl.*, vol. 31, no. 2, pp. 419–428, 1995, doi: 10.1109/28.370294.

[8] C. K. Morehouse, R. Glicksman, and G. S. Lozier, “Batteries,” *Proc. IRE*, vol. 46, no. 8, pp. 1462–1483, 1958, doi: 10.1109/JRPROC.1958.286968.

[9] I. Honma, “All solid state LIB for mobile applications,” *16th Int. Conf. Nanotechnol. - IEEE NANO 2016*, pp. 836–837, 2016, doi: 10.1109/NANO.2016.7751542.

[10] A. M. Kannan, V. Renugopalakrishnan, S. Filipek, P. Li, G. F. Audette, and L. Munukutla, “Bio-batteries and bio-fuel cells: Leveraging on electronic charge transfer proteins,” *J. Nanosci. Nanotechnol.*, vol. 9, no. 3, pp. 1665–1678, 2009, doi: 10.1166/jnn.2009.SI03.

[11] M. Mohammadifar, Y. Gao, and S. Choi, “An origami-inspired multicell biobattery stack,” *Proc. IEEE Sensors*, pp. 9–11, 2017, doi: 10.1109/ICSENS.2016.7808946.

[12] C. Zou, X. Hu, Z. Wei, T. Wik, and B. Egardt, “Electrochemical Estimation and Control for Lithium-Ion Battery Health-Aware Fast Charging,” *IEEE Trans. Ind. Electron.*, vol. 65, no. 8, pp. 6635–6645, 2018, doi: 10.1109/TIE.2017.2772154.

[13] R. O. Ph, “No 主観的健康感を中心とした在宅高齢者における 健康関連指標に関する共分散構造分析Title.”

[14] J. B. Bates *et al.*, “Thin-film rechargeable lithium batteries,” *J. Power Sources*, vol. 54, no. 1, pp. 58–62, 1995, doi: 10.1016/0378-7753(94)02040-A.

[15] C. Brivio, V. Musolino, P. J. Alet, M. Merlo, A. Hutter, and C. Ballif, “Analysis of lithium-ion cells performance, through novel test protocol for stationary applications,” *2017 6th Int. Conf. Clean Electr. Power Renew. Energy Resour. Impact, ICCEP 2017*, no. LiC, pp. 410–415, 2017, doi: 10.1109/ICCEP.2017.8004848.

[16] M. U. Ali, A. Zafar, S. H. Nengroo, S. Hussain, M. J. Alvi, and H. J. Kim, *Towards a smarter battery management system for electric vehicle applications: A critical review of lithium-ion battery state of charge estimation*, vol. 12, no. 3. 2019.

[17] K. A. Smith, “Electrochemical Control of Lithium-Ion Batteries [Applications of Control],” *IEEE Control Syst.*, vol. 30, no. 2, pp. 18–25, 2010, doi: 10.1109/mcs.2010.935882.

[18] R. Sousa, J. A. Sousa, J. F. Ribeiro, L. M. Goncalves, and J. H. Correia, “All-solid-state batteries: An overview for bio applications,” *3rd Port. Bioeng. Meet. ENBENG 2013 - B. Proc.*, 2013, doi: 10.1109/ENBENG.2013.6518400.

[19] F. Yang, X. Song, F. Xu, and K. L. Tsui, “State-of-Charge Estimation of Lithium-Ion Batteries via Long Short-Term Memory Network,” *IEEE Access*, vol. 7, pp. 53792–53799, 2019, doi: 10.1109/ACCESS.2019.2912803.

[20] S. Pang, J. Farrell, J. Du, and M. Barth, “Battery state-of-charge estimation,” *Proc. Am. Control Conf.*, vol. 2, pp. 1644–1649, 2001, doi: 10.1109/acc.2001.945964.

[21] Y. Zou, X. Hu, H. Ma, and S. E. Li, “Combined State of Charge and State of Health estimation over lithium-ion battery cell cycle lifespan for electric vehicles,” *J. Power Sources*, vol. 273, no. January, pp. 793–803, 2015, doi: 10.1016/j.jpowsour.2014.09.146.

[22] P. KI, D. Rao B, and A. Sharma, “Estimation of SOC and SOH of Li-Ion Batteries,” *Int. J. Comput. Appl.*, vol. 104, no. 4, pp. 45–49,

2014, doi: 10.5120/18194-9111.

[23] M. Zhang and X. Fan, "Review on the state of charge estimation methods for electric vehicle battery," *World Electr. Veh. J.*, vol. 11, no. 1, pp. 1–17, 2020, doi: 10.3390/WEVJ11010023.

[24] R. M. Spotnitz, "Battery modeling," *Electrochem. Soc. Interface*, vol. 14, no. 4, pp. 39–42, 2005, doi: 10.1002/9781118970553.ch12.

[25] X. Hu, S. Li, and H. Peng, "A comparative study of equivalent circuit models for Li-ion batteries," *J. Power Sources*, vol. 198, pp. 359–367, 2012, doi: 10.1016/j.jpowsour.2011.10.013.

[26] M. R. Jongerden and B. R. Haverkort, "Which battery model to use?," *IET Softw.*, vol. 3, no. 6, pp. 445–457, 2009, doi: 10.1049/iet-sen.2009.0001.

[27] K. Smith, Y. Shi, and S. Santhanagopalan, "American Control Conference Palmer House Hilton," pp. 728–730, 2015.

[28] C. Zou, A. G. Kallapur, C. Manzie, and D. Nesic, "PDE battery model simplification for SOC and SOH estimator design," *Proc. IEEE Conf. Decis. Control*, vol. 54rd IEEE, no. Cdc, pp. 1328–1333, 2015, doi: 10.1109/CDC.2015.7402395.

[29] M. Jongerden and B. Haverkort, "Battery aging and the Kinetic Battery Model," 2016.

[30] P. Rong and M. Pedram, "An analytical model for predicting the remaining battery capacity of lithium-ion batteries," *Proc. -Design, Autom. Test Eur. DATE*, pp. 1148–1149, 2003, doi: 10.1109/DATE.2003.1253775.

[31] S. X. Tang, L. Camacho-Solorio, Y. Wang, and M. Krstic, "State-of-Charge estimation from a thermal–electrochemical model of lithium-ion batteries," *Automatica*, vol. 83, pp. 206–219, 2017, doi: 10.1016/j.automatica.2017.06.030.

[32] M. Mastali, J. Vazquez-Arenas, R. Fraser, M. Fowler, S. Afshar, and M. Stevens, "Battery state of the charge estimation using Kalman filtering," *J. Power Sources*, vol. 239, pp. 294–307, 2013, doi: 10.1016/j.jpowsour.2013.03.131.

[33] C. Y. Chun, G. S. Seo, S. H. Yoon, and B. H. Cho, "State-of-charge estimation for lithium-ion battery pack using a reconstructed open-circuit-voltage curve," *2014 Int. Power Electron. Conf. IPEC-Hiroshima - ECCE Asia 2014*, pp. 2272–2276, 2014, doi: 10.1109/IPEC.2014.6869906.

[34] S. Sato and A. Kawamura, "A new estimation method of state of charge using terminal voltage and internal resistance for lead acid battery," *Proc. Power Convers. Conf. 2002, PCC-Osaka 2002*, vol. 2, no. 3, pp. 565–570, 2002, doi: 10.1109/PCC.2002.997578.

[35] P. Spagnol, S. Rossi, and S. M. Savaresi, "Kalman Filter SoC estimation for Li-Ion batteries," *Proc. IEEE Int. Conf. Control Appl.*, pp. 587–592, 2011, doi: 10.1109/CCA.2011.6044480.

[36] K. S. Ng, Y. F. Huang, C. S. Moo, and Y. C. Hsieh, "An enhanced coulomb counting method for estimating state-of-charge and state-of-health of lead-acid batteries," *INTELEC, Int. Telecommun. Energy Conf.*, pp. 2–6, 2009, doi: 10.1109/INTLEC.2009.5351796.

[37] A. Farahani, E. Nazemi, G. Cabri, and A. Rafizadeh, "An evaluation method for Self-Adaptive systems," *2016 IEEE Int. Conf. Syst. Man, Cybern. SMC 2016 - Conf. Proc.*, pp. 2814–2820, 2017, doi: 10.1109/SMC.2016.7844665.

[38] G. Hongyu, J. Jiuchun, and W. Zhanguo, "Estimating the state of charge for Ni-MH battery in HEV by RBF neural network," *2009 Int. Work. Intell. Syst. Appl. ISA 2009*, pp. 2–5, 2009, doi: 10.1109/IWISA.2009.5072852.

[39] F. K. Wang and T. Mamo, "A hybrid model based on support vector regression and differential evolution for remaining useful lifetime prediction of lithium-ion batteries," *J. Power Sources*, vol. 401, no. August, pp. 49–54, 2018, doi: 10.1016/j.jpowsour.2018.08.073.

[40] M. W. Yatsui and H. Bai, "Kalman filter based state-of-charge estimation for lithium-ion batteries in hybrid electric vehicles using pulse charging," *2011 IEEE Veh. Power Propuls. Conf. VPPC 2011*, 2011, doi: 10.1109/VPPC.2011.6042988.

[41] W. Wang and J. Mu, "State of Charge Estimation for Lithium-Ion Battery in Electric Vehicle Based on Kalman Filter Considering Model Error," *IEEE Access*, vol. 7, pp. 29223–29235, 2019, doi: 10.1109/ACCESS.2019.2895377.

[42] B. Xia *et al.*, "Strong tracking of a h-infinity filter in lithium-ion battery state of charge estimation," *Energies*, vol. 11, no. 6, p. 121693718, 2018, doi: 10.3390/en11061481.

[43] Z. Liu, X. Dang, and H. Sun, "Online state of charge estimation for lithium-ion battery by combining incremental autoregressive and moving average modeling with adaptive h-infinity filter," *Math. Probl. Eng.*, vol. 2018, 2018, doi: 10.1155/2018/7480602.

[44] J. Xie, J. Ma, and K. Bai, "Enhanced coulomb counting method for state-of-charge estimation of lithium-ion batteries based on peukert's law and coulombic efficiency," *J. Power Electron.*, vol. 18, no. 3, pp. 910–922, 2018, doi: 10.6113/JPE.2018.18.3.910.

[45] R. Zhang *et al.*, "A study on the open circuit voltage and state of charge characterization of high capacity lithium-ion battery under different temperature," *Energies*, vol. 11, no. 9, 2018, doi: 10.3390/en11092408.

[46] Y. Pei, S. Biswas, D. S. Fussell, and K. Pingali, "An elementary introduction to Kalman filtering," *Commun. ACM*, vol. 62, no. 11, pp. 122–133, 2019, doi: 10.1145/3363294.

[47] Q. Li, R. Li, K. Ji, and W. Dai, "Kalman filter and its application," *Proc. - 8th Int. Conf. Intell. Networks Intell. Syst. ICINIS 2015*, no. 10, pp. 74–77, 2016, doi: 10.1109/ICINIS.2015.35.

[48] G. Welch and G. Bishop, "An Introduction to the Kalman Filter," *In Pract.*, vol. 7, no. 1, pp. 1–16, 2006, doi: 10.1.1.117.6808.

[49] F. Yang, Y. Feng, B. Pan, R. Wan, and J. Wang, "State of Charge estimation of lithium ion battery based on extended Kalman filtering algorithm," *IOP Conf. Ser. Earth Environ. Sci.*, vol. 81, no. 1, 2017, doi: 10.1088/1755-1315/81/1/012182.

[50] T. Huria, M. Ceraolo, J. Gazzarri, and R. Jackey, "Simplified extended kalman filter observer for SOC estimation of commercial power-oriented LFP lithium battery cells," *SAE Tech. Pap.*, vol. 2, 2013, doi: 10.4271/2013-01-1544.

[51] S. C. L. Da Costa, A. S. Araujo, and A. D. S. Carvalho, "Battery State of Charge estimation using Extended Kalman Filter," *2016 Int. Symp. Power Electron. Electr. Drives, Autom. Motion, SPEEDAM 2016*, pp. 1085–1092, 2016, doi: 10.1109/SPEEDAM.2016.7525904.

[52] Y. Liu, Y. Huangfu, R. Ma, L. Xu, D. Zhao, and J. Wei, "State of Charge Estimation of Lithium-ion Batteries Electrochemical Model with Extended Kalman Filter," *2019 IEEE Ind. Appl. Soc. Annu. Meet. IAS 2019*, pp. 1–7, 2019, doi: 10.1109/IAS.2019.8911931.

[53] E. A. Wan and R. Van Der Merwe, "The unscented Kalman filter for nonlinear estimation," *Adapt. Syst. Signal Process. Commun. Control Symp. 2000. AS-SPCC. IEEE 2000*, no. 3, pp. 153–158, 2002.

[54] W. Wang, X. Wang, C. Xiang, C. Wei, and Y. Zhao, "Unscented kalman filter-based battery SOC estimation and peak power prediction method for power distribution of hybrid electric vehicles," *IEEE Access*, vol. 6, no. c, pp. 35957–35965, 2018, doi: 10.1109/ACCESS.2018.2850743.

[55] T. Xiao, X. Shi, B. Zhou, and X. Wang, "Comparative Study of EKF and UKF for SOC Estimation of Lithium-ion Batteries," *2019 IEEE PES Innov. Smart Grid Technol. Asia, ISGT 2019*, no. 51707108, pp. 1570–1575, 2019, doi: 10.1109/ISGT-Asia.2019.8880915.

[56] G. L. Plett, "Sigma-point Kalman filtering for battery management systems of LiPB-based HEV battery packs. Part 2: Simultaneous state and parameter estimation," *J. Power Sources*, vol. 161, no. 2, pp. 1369–1384, 2006, doi: 10.1016/j.jpowsour.2006.06.004.

[57] M. Zhang, K. Wang, and Y. T. Zhou, "Online state of charge estimation of lithium-ion cells using particle filter-based hybrid filtering approach," *Complexity*, vol. 2020, 2020, doi: 10.1155/2020/8231243.

[58] S. Sitjongsataporn and T. Wiangtong, "S. SITJONGSATAPORN et al.: ANALYSIS OF REDUCED COMPLEXITY WIDELY-LINEAR Analysis of Reduced Complexity Widely-Linear Adaptive Forgetting-Factor Inverse Square-Root Recursive Least Squares algorithm."

[59] Z. He, Z. Yang, X. Cui, and E. Li, "A Method of State-of-Charge Estimation for EV Power Lithium-Ion Battery Using a Novel Adaptive Extended Kalman Filter," IEEE Trans Veh Technol, vol. 69, no. 12, pp. 14618–14630, Dec. 2020, doi: 10.1109/TVT.2020.3032201.

[60] IEEE Malaysia Section, IEEE Region 10., and Institute of Electrical and Electronics Engineers, Proc. of the 2017 IEEE Region 10 Conference (TENCON), Malaysia, November 5-8, 2017.
[61] Rimsha et al., “State of charge estimation and error analysis of lithium-ion batteries for electric vehicles using Kalman filter and deep neural network,” J Energy Storage, vol. 72, Nov. 2023, doi: 10.1016/j.est.2023.108039.
[62] A. K. P, P. K. S, M. K. A, S. B. S, P. B. D, and D. K. R, “Recurrent Neural Network based Data-Driven SOC Estimation in Lithium-Ion Battery,” Institute of Electrical and Electronics Engineers (IEEE), Jun. 2023, pp. 1–6. doi:10.1109/icdcece57866.2023.10150795.